Development, Modeling, and Testing of a Unified Controller for Prosumers Connected to 0.4 kV Voltage Level Grids. Part II: Experimental Validation

I. Idrisov[1], Y. Vlasov[1], M. Korzhavin[2], A.N. Stadnikov[3], F. M. Ibanez[1], V. Kononenko[3], P. Vorobev[1,*]

[1]Skolkovo Institute of Science and Technology, Moscow, Russia
[2]Foundation "National Intellectual Resource", Moscow, Russia
[3]Rosseti Science and Technology Center, Moscow, Russia

***Abstract* — In this second part of the study we present the results of a laboratory testing of the performance of our unified prosumer controller. Complex multi-timescale dynamics of power electronics devices makes it crucial to perform the experimental validation of our findings [1, 2]. First, we describe the control system of inverters that are used in the testing. These inverters were designed and assembled by us specifically to have extended control capabilities compared to commercially available inverters. In fact, we have the full access to any of the control loops of those inverters – from the power stage and pulse-width modulation (PWM) realization to grid synchronization and slowly acting power control. We then proceed to the laboratory testing of the controller performance. First, we test the power setpoints control for prosumers in a closed-loop setup when the unified controller reassigns the setpoints for prosumers following a sudden change in the loads of the feeder. Next, we proceed to a more challenging task of a seamless transition of the grid into islanded operation. To this end, upon detection of the event of disconnection for the main substation, the unified controller assigns one of the prosumers to transition to a grid-forming mode. Thus, there is no interruption of the power supply after disconnection from the main grid. Finally, we demonstrate the reverse transition when the islanded grid is connected back to the feeding substation.**

***Index Terms*: prosumers, inverters, distribution grids, control of multiple energy sources.**

* Corresponding author.
E-mail: p.vorobev@skotech.ru

http://dx.doi.org/10.38028/esr.2021.04.0002
Received november 26, 2021. Accepted December 28, 2021.
Available online January 25, 2022.

I. Introduction

Coordinated control of prosumers connected to a distribution grid can offer a lot of advantages from the point of view of the grid operating conditions. A number of advantages can be brought by coordinated control to grids with low to moderate prosumer percentage: better voltage regulation, minimization of power losses, avoiding line overloads, to name a few typical examples. For the grids with a high percentage of prosumers among the loads, coordinated control can become a necessity – the uncoordinated actions of multiple prosumers will often drive the grid into unacceptable operating states. Moreover, for grids with enough generation capabilities to satisfy the load, it is possible to perform a transition to islanded operation, when the feeder disconnects from the main grid, while still operating and feeding all the loads. In this case, at least one of the inverters should switch into the grid-forming mode, and this can be realized with the help of a unified controller.

Although there are a lot of different control algorithms proposed in literature, most of the results concern some optimal energy management systems with the addition of reactive power dispatch. The validation is usually done by simple power flow type simulations, without taking into account the complex nature of the prosumer power electronics interfaces. In this second part of the study, we present the results of the laboratory testing of our new unified controller for prosumers. We perform the tests based on the smart grid laboratory setup, supplemented by additional high-resolution measurement system and custom-made inverters connected to the test bench. This type of experimental validation provides an ultimate way of testing the validity of our controller design. The test bench provides a very realistic replication of a real-life distribution feeder, and experimental results serve as the first step towards commercial-scale implementation of the unified controller.

For our testing purposes, we have pre-selected a number of specific scenarios, ranging from simple

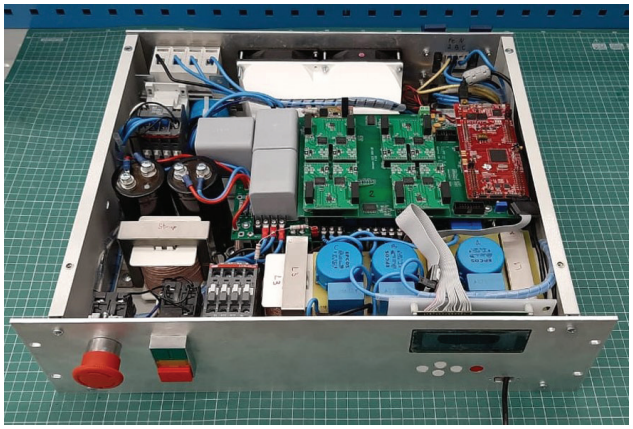

Fig. 1. A photographic image of the inverter developed and assembled in our laboratory for validation testing of the unified prosumer controller.

power setpoint adjustments to fast transitions between grid-following and grid-forming modes for inverters. Three inverters with fully "open" control system have been developed and assembled specifically to perform the experimental validation of the unified controller. In Section II, we provide a detailed description of the inverters, including hardware design and control loops implementation. Section III then proceeds to describe the actual testing. Two complex test scenarios have been investigated. The first one focuses on an automatic change of power (both active and reactive) setpoints of prosumers following a sudden load change in the feeder. The second one is dedicated to a seamless transition to islanded operation and back to the grid-connected operation without interrupting the load supply. This is done by a fast action of the unified controller that sends a signal to one of the prosumers to switch between grid-following and grid-forming modes of operation.

II. Inverters used for representation of prosumers

In this section we provide a description of inverters that were designed and assembled specifically to be used in laboratory tests, including the validation of the unified controller operation. The main advantage of the self-designed inverters over commercial ones is that the control system of the inverters is fully accessible to us.

A photographic image of one of the inverters is shown in Fig. 1. The maximum power rating of the inverter is 5 kW. The power stage is realized by the Semikron SKiiP 24NAB126V10 module that contains 7 IGBTs, 6 of which form 3 half-bridge modules, and the 7th one is used for the boost-converter function at the DC-side. Three ISO5852 cards are used as gate drives. The LAUNCHXL-F28379D board with 2-core DSP processor TMS320F2837xD (200 MHz) is used to execute the control algorithms, including PWM, current controller, voltage controller, and/or phase-locked-loop.

The control system for inverters was realized in two different modes: the grid-following mode and the grid-forming one [3]. The flowchart of control systems for the two modes are presented in Fig. 2 and Fig. 3, respectively. Both control modes have the same arrangement of the power stage and the current controller. The grid-following mode also has the phase-locked-loop control block that measures the grid frequency and phase, while the grid-forming mode has the voltage control block instead, which sets the voltage setpoint for the inverter [4].

For both operating modes the power stage control is realized by sinusoidal pulse-width modulation (PWM) [5, 6] with a switching frequency of 20 kHz. Other PWM strategies are also possible, such as third harmonics injection of space vector modulation (SVM), however, they influence only the harmonic content of the inverter current and have minimal effect on the rest of the control systems.

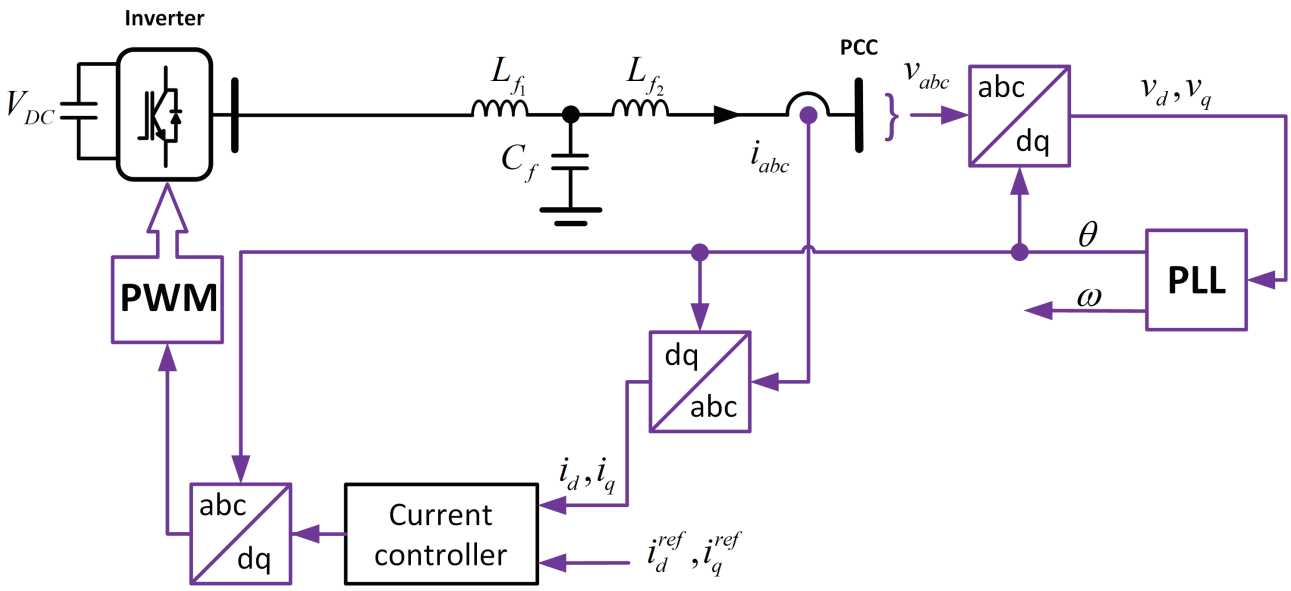

Fig. 2. Flowchart of the inverter control system in the grid-following mode.

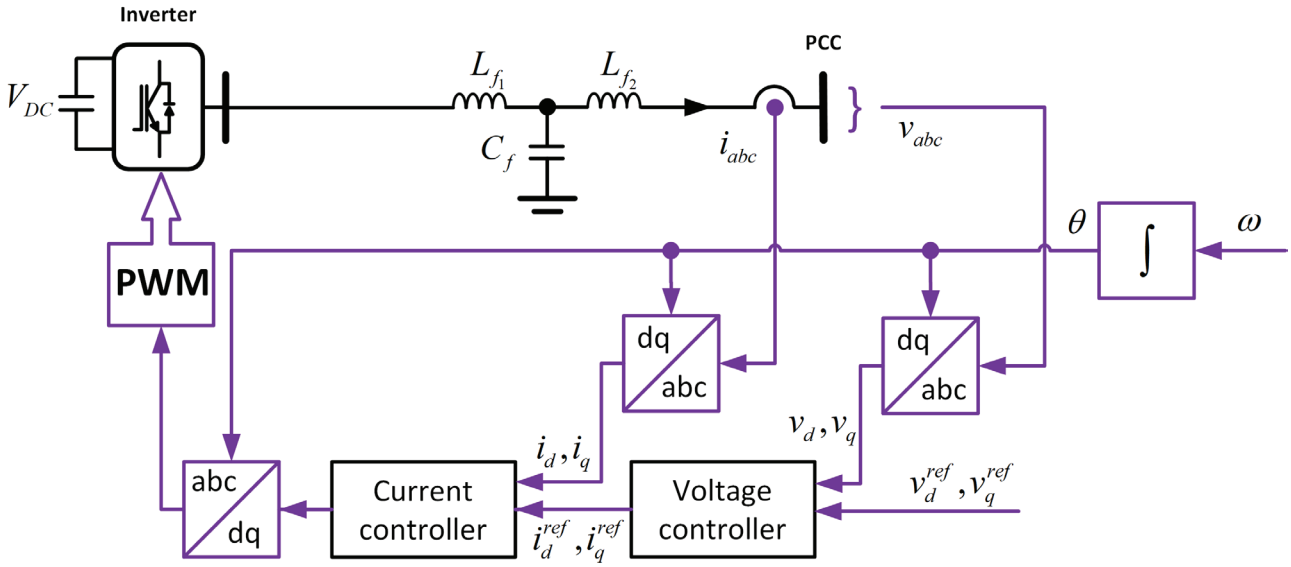

Fig. 3. Flowchart of the inverter control system in the grid-following mode.

The current controller follows a typical $D - Q$ decoupling scheme [3] with a PI controller chosen so as to compensate for the EM-filter dynamics. The bandwidth of the current controller is chosen to be 1 ms. In the grid-following mode of operation, the current controller receives the setpoints for the real and reactive currents i_d^* and i_q^* from the unified prosumer controller. While in the grid-forming mode, the current controller setpoints are received from the voltage control loop of that same inverter.

For the grid-following mode, a phase-locked-loop (PLL) block measures the grid voltage and phase and sends the signals to the current controller and PWM. A standard decoupled double reference frame (DDSRF) PLL is implemented [7] due to its good performance under unbalanced conditions [8]. For the grid-forming mode, the feedback voltage controller [3, 4] is used, for which the voltage reference signal v_d^* and v_q^* is set to be constant. The voltage controller then generates the setpoints i_d^* and i_q^* for the current controller. Both grid-following and grid-forming modes can operate in all 4 quadrants with an arbitrary combination of real and reactive power injection/consumption within the capability curve of the inverter.

III. Validation of controller performance

In this section we present the results of the validation of the unified controller performance by hardware experiments. In order to demonstrate the controller capabilities, a number of controller actions was tested, from simple adjustment of prosumers' setpoints for real and reactive power to a seamless transition of the feeder between islanded and grid-connected operation.

The experimental validation is done using the test bench, described in Part I of the study, which is shown here in more details in Fig. 4. The controller takes high-resolution (20 kHz) measurements from the "ADC" block near the connection to the feeding transformer. Measurements from all the other buses are made at a lower resolution (5–50 Hz). For validation of the controller capabilities, two complex experimental scenarios are realized. Scenario 1 is designed to check the controller ability to update the power setpoints of prosumers following sudden changes in the feeder loading level. Scenario 2 is dedicated to a seamless transition of the feeder between islanded and grid-connected operation. One can view Scenario 1 as testing of "slow" control actions, those taken over a period of several seconds, and Scenario 2 as testing of fast control actions, those taken over a period of several milliseconds. In the latter case, the unified controller's goal is to provide a seamless transition between grid-connected and islanded operation (and back) by quickly reassigning the grid-forming operating mode to one of the inverters once the disconnection from the feeding transformer is detected. The process should be executed in such a way that the load supply is not interrupted.

A. Scenario 1: adjustment of prosumers' power setpoints

In this scenario, we test how the unified controller is able to respond to a sudden load step-change by readjusting the power setpoints of prosumers in such a way so as to keep the (active) power drawn from the feeding transformer constant. Scenario 1 proceeds as follows:

1. The feeder is in the grid-connected mode with no loads initially. Three prosumers are connected to the feeder as shown in Fig. 4. Prosumer 2 operates at the constant power setpoint and is not managed by the unified controller. Prosumers 1 and 3 are initially at the zero-power output (both active and reactive) and managed by the unified controller.
2. An active load of 350 W in each phase is connected at the Load 2 bus, and the unified controller detects the change in the power flow at the input to the feeder.

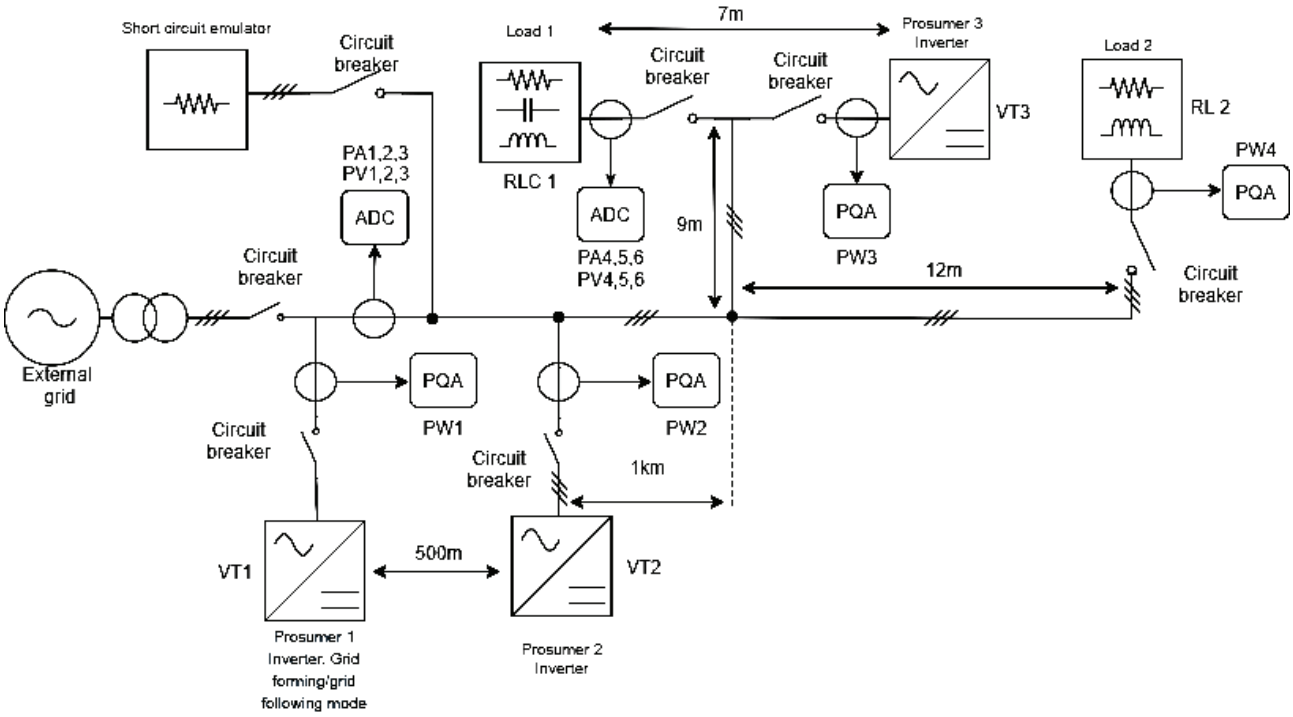

Fig. 4. Single-line diagram of the test bench with loads, prosumers, and the measurement system mounted.

The power setpoints of Prosumers 1 and 3 are then readjusted by the unified controller.

3. After the feeder comes to a new steady-state, a reactive load of 250 VAr in each phase is connected at the Load 2 bus, and the unified controller readjusts the reactive power setpoints of the prosumers in response.

The active powers consumed by the load and drawn from the feeding during the first experiment is shown in Fig. 5. The data is taken from the SCADA system of the test bench. We note that the initial real power drawn by the feeder from the grid is not zero (approximately 200 W), although the loads are not connected to the feeder, which is due to the test bench auxiliary equipment demand. We keep this power constant during the experiments. From Fig. 5 we see that at the moment of time t = 3 905 s a sudden load growth happens (green line) within the next several seconds (load connection is automatically managed by the test bench internal control system, following our manual signal). Likewise, the power drawn from the feeding transformer (orange line) is also increased accordingly during the first seconds. However, after the first few seconds, the unified controller starts to gradually change the prosumers' power setpoints and within about 15 seconds from the initial load step-change the controller is able to restore the active power drawn by the feeder from the grid to its pre-disturbance value. Such a speed of response is more than enough to deal with the possible over-current in the feeder lines and prevent any excessive line heating.

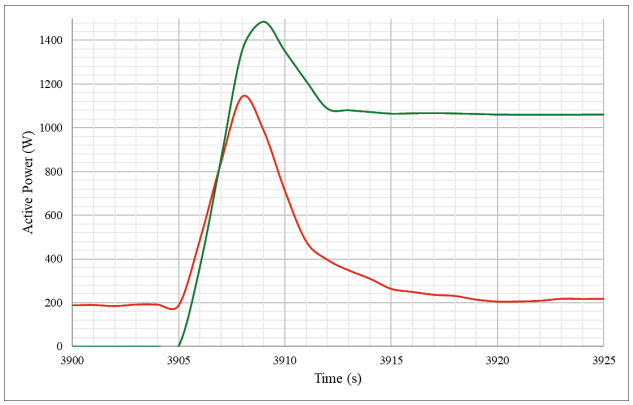

Fig. 5. Change of the active power total load (green) and the active power flow from the feeding substation (orange) after the load increase and subsequent action of the unified controller that changes the power setpoints of prosumers.

More details on how the controller changes the prosumers' active power set-points can be seen at the oscillograms in Fig. 6. Here, the top panel (yellow) shows the feeder voltage and the middle and bottom panels (green and blue) show the currents of prosumers – green stands for Prosumer 3, and blue stands for Prosumer 1. It can be seen that initially, following a load step up, the controller commands both prosumers to increase their power output in order to quickly restore the feeder current back to its pre-disturbance value. However, during the next several seconds the controller is performing a re-distribution of the active power generation between Prosumers 1 and 3 in such a way as to minimize voltage deviation from the rated one on the feeder buses. This leads to Prosumer 3 taking almost all the excessive load and Prosumer 1 restoring its power output to almost the pre-disturbance value (nearly zero).

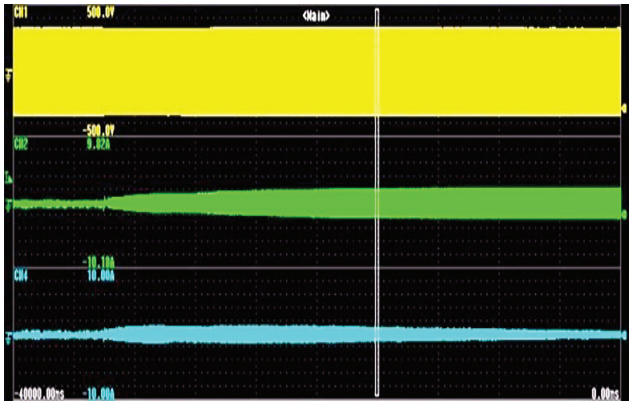

Fig. 6. Oscillograms of the feeder voltage (yellow) and currents of Prosumers 3 (green) and 1 (blue) during the active load increase in the feeder and the consequent unified controller action. It can be seen that the unified controller is compensating for the load increase predominately by increasing the active power setpoint of Prosumer 3.

This is reasonable since the load step change occurred on a bus that is the closest to Prosumer 3, so changing the power output of the closest prosumer induces the least voltage disturbance and the least excessive power flows over the lines in the feeder.

After the transient response to an active load change settles, another disturbance is applied – this time a sudden increase in the reactive load on Load bus 2 (250 VAr for each phase). As in the previous case the controller executes the readjustment of the (reactive) power setpoints of the two prosumers under control. The reactive power drawn from the grid and consumed by the load during the whole process is shown in Fig. 7, which is based on the SCADA system data. As in the previous case, immediately following the sudden increase in the reactive power demand by the load, the reactive power drawn from the grid increases, but then the controller starts to readjust the prosumers' reactive power output, which leads to a change in the reactive power drawn from the feeding transformer within the next several seconds. However, unlike in the case of real power, the reactive power consumption by the feeder is not returned back to the exact pre-disturbance value, but a slight reactive power over-compensation is observed, which is the result of the controller finding the optimal operating point in terms of both power flow and the feeder voltage profile.

Fig. 8 shows oscillograms of the feeder voltage and prosumers' current, where the notation used is the same as for Fig. 6. The process of a reactive power load change starts from the operating point, where the active power output of Prosumer 3 is already substantial (in order to compensate for the previous active load increase) and this can be observed from the middle panel of Fig. 8. In this case, the reactive power setpoint increase is mostly done for Prosumer 3 with little participation of Prosumer 1 even during the transient. Since the increase of the reactive power output of Prosumer 3 is performed already on top of a rather high active power output, it does not lead to a substantial change in the prosumer output current amplitude, so that the oscillogram does not show a very distinct change in the current amplitude.

Overall, the unified controller was able to successfully respond to sudden changes in active and reactive power demands in the feeder and re-adjusted the prosumers' power outputs in order to compensate for the load increase. In both cases of active and reactive power demand increases, the controller drove the total feeder power demand back to

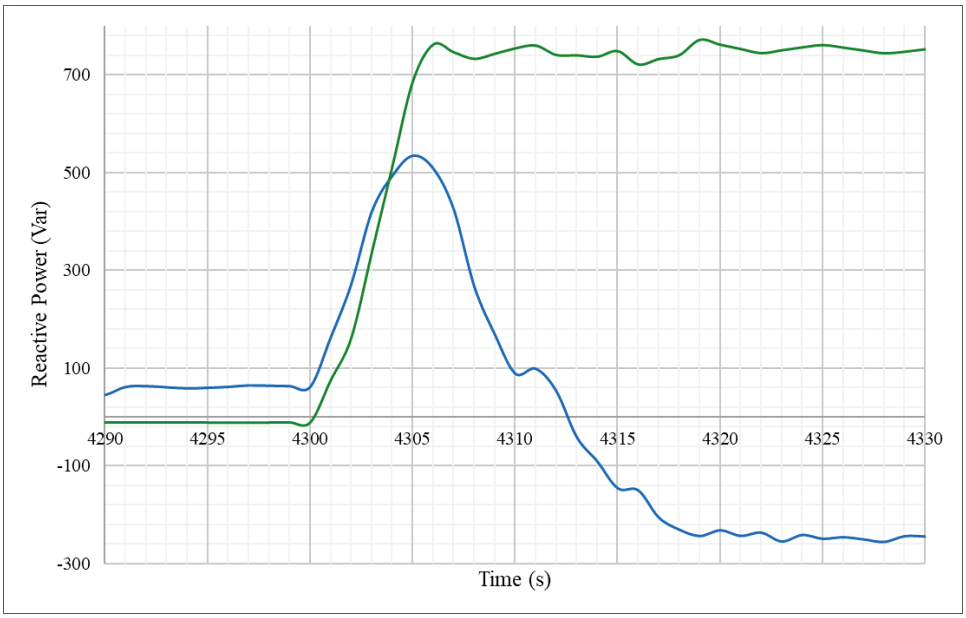

Fig. 7. Change in the active power total load (green) and the active power flow from the feeding substation (orange) after a load increase and subsequent action of the unified controller that changes the power setpoints of prosumers.

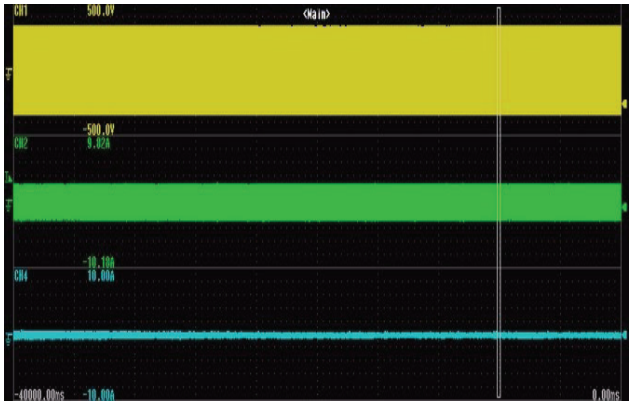

Fig. 8. Oscillograms of the feeder voltage (yellow) and currents of Prosumers 3 (green) and 1 (blue) during a reactive load increase in the feeder and the consequent unified controller action. The excessive reactive power is drawn predominantly from Prosumer 3.

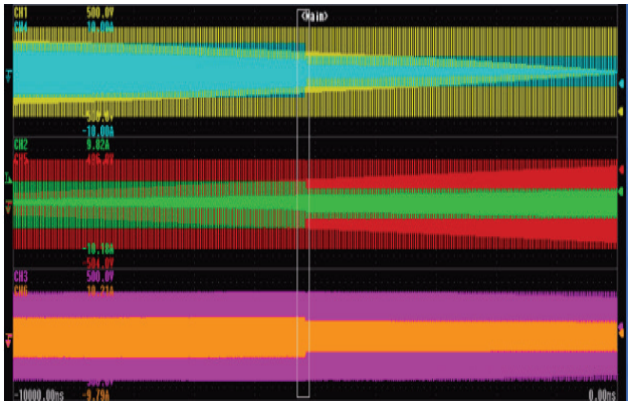

Fig. 9. Transition of the feeder from the grid-connected to islanded operation. Three panels show the voltage and current oscillograms from the three phases of Prosumer 1 inverter that transitions in the grid-forming mode once the islanding is detected.

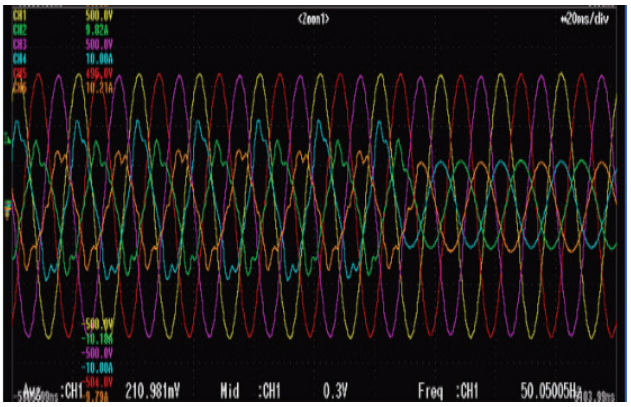

Fig. 10. Detailed oscillograms of the voltage and currents in three phases of the inverter of Prosumer 1 when it goes to islanded operation. The seamless transition is clearly visible for there is no interruption in either current or voltage.

the pre-disturbance values (apart from some slight over-compensation of reactive power) within 10-20 seconds following the load disturbance. This is more than enough to correct any possible violation of the maximum current limits in feeder lines that might happen if the prosumers' control is uncoordinated (or excessive loading occurs). In addition to correcting the power flows, the controller also distributes the real and reactive power loading between the prosumers in such a way as to minimize voltage variations on the feeder buses, so that the prosumer closest to the load disturbance takes the most responsibility. The entire control is implemented in a fully automated way with feedback loops from the measurement system and without any manual intervention (apart from the signals to emulate a load disturbance).

B. Scenario 2: transition from the grid-connected to islanded operation and back

Let us now turn to testing a much more challenging control action: a seamless transition of a feeder under non-zero loading from the grid-connected to islanded operation and back. What is important is that the transition should be done in such a way as to avoid any possible load interruption. For this purpose, at least one of the prosumer inverters should be switched over to the grid-forming mode immediately after the disconnection from the main grid occurs. In our case, this will be Prosumer 1, which can switch between those two modes following the corresponding commands from the unified controller.

In order to test the transition to islanded operation we perform an intentional disconnection of the feeder from the external grid, while the unified controller is in its normal operating state. Once the islanding is detected by the controller, a command is sent to Prosumer 1 to switch its inverter to the grid-forming mode, so that the feeder can continue to operate even without the connection to the external grid. After certain time of the operation in the islanded mode, the reverse transition is initiated by the unified controller commanding Prosumer 1 to switch back to the grid-following mode once the connection to the main grid is detected. Thus, Scenario 2 proceeds as follows:

1. The feeder is in the grid-connected mode with the overall loading of 350 W per phase which is connected at the Load 2 bus. Three prosumers are connected to the feeder as shown in Fig. 4. Prosumer 2 operates at the constant power setpoint (equal to zero) and is not managed by the unified controller. Prosumers 1 and 3 are initially at the zero-power output (both active and reactive) and managed by the unified controller.
2. While the unified controller is in the normal operating state, the feeder is suddenly disconnected from the external grid by tripping of the corresponding circuit breaker. The controller automatically detects the islanding event and sends the corresponding command to Prosumer 1 for switching to the grid-forming mode. An additional command is sent to Prosumer 3 to change its active power output.
3. Prosumer 1 switches to the grid-forming mode, while Prosumer 3 also adjusts its power output, so that the load is fed without any interruption.

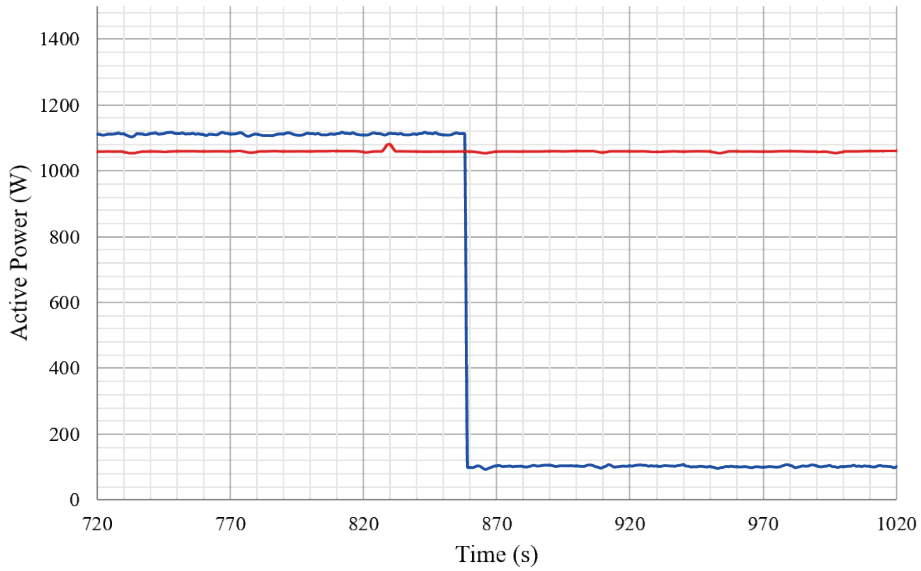

Fig. 11. Active power supplied to the load (orange curve) and consumed from the grid (blue curve) during the process of transition between grid-connected and islanded operation.

4. After some time of the islanded operation (about 5 minutes) the external grid voltage is back, and the feeder can be reconnected. Upon observing the normal grid voltage, the controller sends the corresponding signals to Prosumer 1 operating in the grid-forming mode in order to adjust the frequency and phase so that a seamless reconnection can take place.
5. The reconnection to the external grid occurs with Prosumer 1 switching back to the grid-following mode with the constant power output (the same as before the islanding). At the same time, the power setpoint of Prosumer 3 is also returned back to the value before the islanding. The load is fully served without any interruption during the entire experiment.

Fig. ***9*** shows the oscillograms of the three phases of the inverter of Prosumer 1 during the process of islanding. It is clear that the transition occurs with a change in the inverter current. Fig. ***10*** shows the actual transition process to the islanding mode in more detail. Here, the oscillograms of voltages and currents in all three phases of the inverter are shown. The transition is clearly visible, and its seamless character can be also seen – there is no discontinuity of any kind in currents in any phase. The inverter currents are slightly distorted by harmonics while in the grid-following mode, but this is the result of some flaws in inverter internal controls and neither affects the unified controller performance nor the transition between grid-following and grid-forming modes.

Fig. ***11*** shows the active power supplied to the load (orange curve) and consumed from the grid (blue curve) during the process of islanding. It is clearly visible that the power drawn from the grid goes to zero (apart from the

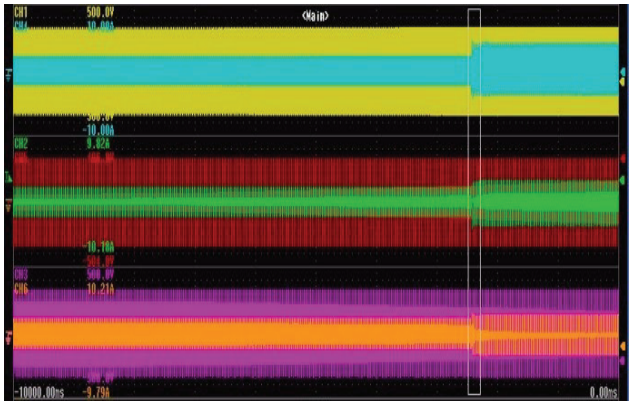

Fig. 12. Transition of the feeder from islanded to grid-connected operation. Three panels show the voltage and current oscillograms from the three phases of the Prosumer 1 inverter that transitions in the grid-following mode once the connection to the external grid is detected.

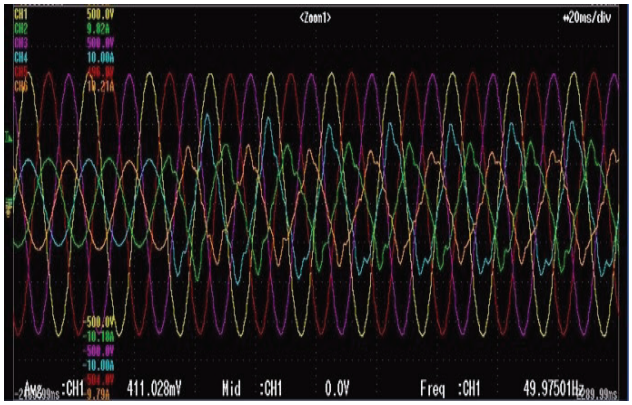

Fig. 13. Detailed oscillograms of the voltage and currents in three phases of the Prosumer 1 inverter 1 when it transitions from islanded to grid-connected operation. The seamless transition is clearly visible for there is no interruption in either current or voltage.

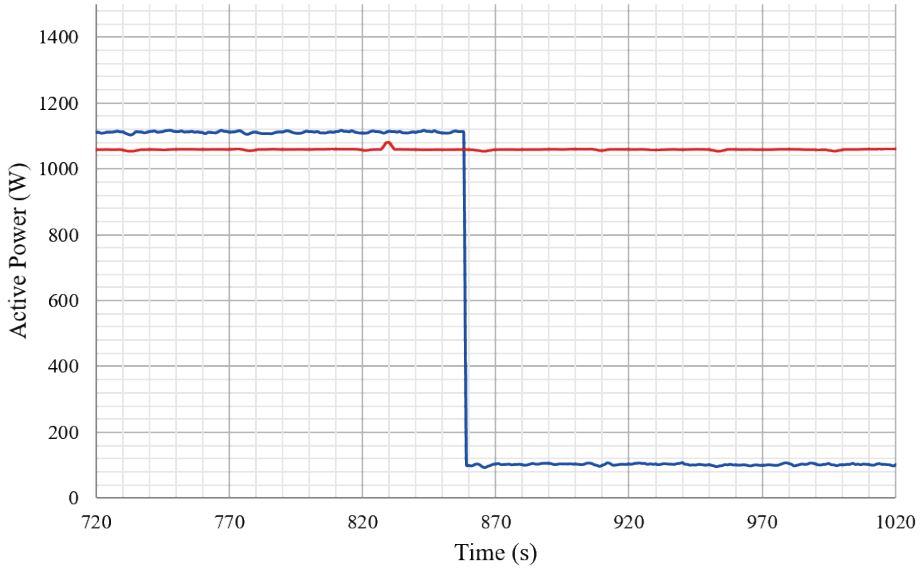

Fig. 14. Active power supplied to the load (orange curve) and consumed from the grid (blue curve) during the process of the transition between islanded and grid-connected operation.

demand on the part of the test bench auxiliary equipment) after the feeder disconnection is performed. However, the load is supplied in an uninterrupted way during the whole process which is guaranteed by the action of the unified controller that has performed the transition of the feeder to islanded operation.

After some time operating in the islanded mode (around 5 minutes) we perform the reconnection of the feeder back to the main grid, with the controller taking care of the seamless transition. Fig. ***12*** shows the oscillograms for the three phases of the inverter of Prosumer 1 during the process of the transition from islanded to grid-connected operation. It is also visible, as in the previous case, that the transition is followed by a change in the inverter RMS current. Fig. ***13*** shows the actual transition process from islanded to grid-connected operation in more detail, where the oscillograms of voltages and currents in all three phases of the inverter are shown. The transition is clearly visible and its seamless nature can be also seen: there is no discontinuity of any kind in currents in any phase.

Finally, Fig. ***14*** shows the active power supplied to the load (orange curve) and consumed from the grid (blue curve) during the process of switching from islanded to grid-connected operation. We see that the power drawn from the grid goes from zero (apart from the demand on the part of the test bench auxiliary equipment) to the load value after the re-connection to the grid is completed. As with the process of islanding, the load is supplied in an uninterrupted way during the whole process which is guaranteed by the action of the unified controller that has performed the transition of the feeder back to grid-connected operation by sending control commands to Prosumer 1 inverter to switch to the grid-following mode, once the re-connection happens.

IV. Conclusion

With power electronics devices becoming more widely available and with the reduction of prices for energy storage and renewable power sources, traditional distribution will undergo significant changes, where conventional consumers will turn into prosumers, grid participants that can both consume and produce power. It is only a matter of time when the wide spread of prosumers and their uncoordinated control will lead to exacerbating the issues of grid security and stability. Thus, there is a need for development of methods for coordinated prosumer control that can be realized in distribution grids. This control can become challenging due to complex dynamics of power electronics devices, so research is needed in order to develop control algorithms and ways of their implementation.

In this two-part study we have presented the unified controller for prosumers connected to 0.4 kV distribution grids. We have described the controller architecture and basic functions, and then performed extensive testing of the controller performance using a laboratory test bench. Our controller has a broad range of possible control actions that it can execute, ranging from rather simple adjustments of power setpoints to seamless transitions between inverter operating modes. Our experimental validation represents a first step towards the commercial-scale controller implementation.

Further research and development can be focused on the design of controllers with different requirement with respect to communications and computational infrastructure. For such applications as power setpoints adjustment possible simplifications can be made, and requirements for sensors and controller performance can be relaxed. Another direction is the possible coordinated control of prosumers connected to different (but adjacent) feeders, which can be realized by some coordinated action of multiple unified controllers acting on different feeders.

Acknowledgements

The project was implemented as a part of the contract with the Rosseti-Centre company.

References

[1] Y. Sun, "The impact of voltage-source-converters' control on the power system: the stability analysis of a power electronics dominant grid," 2018.

[2] Vorobev, P.-H. Huang, M. Al Hosani, J. L. Kirtley, and K. Turitsyn, "High-fidelity model order reduction for microgrids stability assessment," *IEEE Transactions on Power Systems*, vol. 33, no. 1, pp. 874–887, 2017.

[3] A. Yazdani and R. Iravani, *Voltage-sourced converters in power systems: modeling, control, and applications*. John Wiley & Sons, 2010.

[4] N. Pogaku, M. Prodanovic, and T. C. Green, "Modeling, analysis and testing of autonomous operation of an inverter-based microgrid," *IEEE Transactions on power electronics*, vol. 22, no. 2, pp. 613–625, 2007.

[5] D. G. Holmes and T. A. Lipo, *Pulse width modulation for power converters: principles and practice*. John Wiley & Sons, 2003, vol. 18.

[6] E. R. C. Da Silva, E. C. dos Santos, and B. Jacobina, "Pulse width modulation strategies," *IEEE Industrial Electronics Magazine*, vol. 5, no. 2, pp. 37–45, 2011.

[7] S. Golestan, J. M. Guerrero, and J. C. Vasquez, "Three-phase PLLs: A review of recent advances," *IEEE Transactions on Power Electronics*, vol. 32, no. 3, pp. 1894–1907, 2016.

[8] R. Teodorescu, M. Liserre, and P. Rodriguez, *Grid converters for photo-voltaic and wind power systems*. John Wiley & Sons, 2011, vol. 29.

Ildar Idrisov graduated from the Nosov State Technical University (MSTU), Magnitogorsk, Russia, in 2014, majoring in Engineering Systems Control. He earned his M.Sc. degree in Automated Control from MSTU in 2017. From 2011 to 2014, he was part of Microtopography Research Center, MSTU. From 2016 to 2018, he worked as Software Developer at the Compass Plus company. Since 2018, he has been working as Software Engineer with the Center of Energy Science and Technology, Skoltech, where he is currently working towards his Ph.D. degree. His research interests center around power inverters and energy storage systems. He is a professional embedded software developer.

Yaroslav Vlasov graduated from the Moscow State University of Railway Engineering (MIIT), Russia, in 2009, majoring in Robotic Systems Engineering. From 2009 to 2017 he served as Senior Lecturer in the same university. During 2016-2018 as Chief Engineer of an industrial company he led the development of power converters. Currently, he is Hardware Developer at the Skolkovo Institute of Science and Technology (Skoltech), Moscow, Russia.

Maksim Korzhavin graduated as a qualified Researcher and Research Instructor from the graduate school of the South Ural State University (National Research University), Chelyabinsk, Russia, in 2020. His research topic is "Microprocessor tools and control systems for multi-level frequency converters". Currently, as part of a research team, he is involved in the project "Development of a power grid controller" supported by the "National Intellectual Development" Foundation for Support of Scientific and Project Activities of Students, Postgraduates, and Young Scientists.

Alexander Stadnikov graduated from the Moscow Engineering Physics Institute in 1992. In 2020, he completed the postgraduate course at the Russian University of Transport, Department of Electric Power Engineering of Transport. Since 1992, he has been working as an engineer in the electric power industry. Currently, he is Chief Expert at the Department of Energy Storage Systems of the Federal Testing Center of Rosseti Scientific and Engineering Center. He has authored 12 research papers on electric power systems.

Federico Martin Ibanez received B.S. degree in Electronic Engineering from the National Technological University (UTN), Buenos Aires, Argentina, in 2008, and his Ph.D. degree in Power Electronics from the University of Navarra, San Sebastian, Spain, in 2012. From 2006 to 2009, he was part of the Department of Electronics, UTN. From 2009 to 2016, he was part of the Power Electronics Group of Centro de Estudios e Investigaciones Tecnicas de Gipuzkoa. He is currently an Assistant Professor at the Center of Energy Systems, Skoltech, Moscow, Russia. His research interests are in the areas of high-power DC/DC and DC/AC converters for applications related to energy storage, supercapacitors, electric vehicles, and smart grids.

Vladimir Kononenko graduated from the Physics and Engineering Faculty of the Ural Polytechnic Institute (currently the Ural Federal University) in 1994, majoring in Nuclear Power Facilities and Electrophysics. In 2009, he received his Ph.D. in Experimental Physics. His research is focused on the development and study of storage and energy conversion systems, including the systems used for research in the field of High Energy Density Physics. Currently, he is a supervisor at Rosseti Scientific and Engineering Center.

Petr Vorobev received his Ph.D. degree in Theoretical Physics from the Landau Institute for Theoretical Physics, Moscow, Russia, in 2010. From 2015 to 2018, he was a Postdoctoral Associate with the Department of Mechanical Engineering, Massachusetts Institute of Technology, Cambridge, MA, USA. Since 2019, he has been an Assistant Professor with the Skolkovo Institute of Science and Technology, Moscow, Russia. His research interests include a broad range of topics related to power system dynamics and control. This covers low-frequency oscillations in power systems, dynamics of power system components, multi-timescale approaches to power system modeling, and development of plug-and-play control architectures for microgrids.